

Penetration depth model for optical alignment of nuclear spins in GaAs

Patrick J. Coles and Jeffrey A. Reimer

Department of Chemical Engineering, University of California, Berkeley, Berkeley, California 94720, USA

(Received 4 June 2007; published 30 November 2007)

A framework for predicting bulk NMR quantities in semi-insulating GaAs under optical alignment conditions is developed by combining literature penetration depth data with simple kinetic equations. The model accounts for the major photoconductivity and NMR intensity variations with photon energy, including the peak near 1.5 eV. With the fitting parameters fixed, the photon-flux dependence of the NMR intensity is predicted quantitatively up to an energy shift. At the highest fluxes, we see the NMR intensity level off, suggesting that it is possible to completely fill the relevant electronic reservoir. The model also quantitatively fits the time dependence of the light-induced hyperfine shift. The experimental and modeling results have implications toward understanding the microscopic mechanism, and are consistent with nuclear polarization via bound electrons. Finally, the model makes experimentally testable predictions for the photon energy and flux dependences of the spin temperature and hyperfine shift of the NMR line.

DOI: [10.1103/PhysRevB.76.174440](https://doi.org/10.1103/PhysRevB.76.174440)

PACS number(s): 76.60.-k, 71.55.Eq, 82.56.Na

I. INTRODUCTION

The solid-state spin refrigerator was first predicted theoretically by Overhauser,¹ then realized by Carver and Slichter² through continuous saturation of the electron-spin transition in metallic particles. The general principle was to alter the electron-spin temperature by continuous application of Zeeman-resonant radiation; then the nuclear spins, being in thermal contact with the electrons, relax to a new temperature that is significantly lower than the lattice's. Lampel demonstrated that similar criteria could be satisfied in a semiconductor under near-band-gap (optical) irradiation.³ Much experimental work ensued to map out the optimal conditions for this optical alignment process in GaAs,^{4,5} InP,^{6,7} CdTe,⁸ and Si,⁹ and even larger spin alignments have been achieved with the optical method than with the original microwave method. Here, we present a model for optical nuclear-spin alignment in bulk GaAs, the semiconductor for which this phenomenon has been most investigated. While nuclear-spin dynamics in this system has been modeled previously,^{5,10} our model combines the spin dynamics with equations for charge carrier excitation, recombination, and occupation of localized states. It provides an explanation for the effect of photon flux and energy on the alignment process.

From a technological perspective, this model may assist efforts to optimize information storage in nuclear-spin systems, as several nuclear-spin quantum computing proposals rely on a period of optical alignment.^{11,12} From a scientific perspective, the most interesting question is what microscopic events ultimately cause the nuclear-spin alignment, a matter of active research even 40 years now since the phenomenon's discovery. The model presented herein provides a framework for the testing of proposed microscopic mechanisms, in that the model outputs are predictions for all quantities measurable by bulk, single-pulse NMR related to this phenomenon. This model may be useful for other inorganic semiconductors, for which macroscopic observations have been used to construct arguments^{8,7} for particular microscopic mechanisms.

The photon-energy dependence of this optically pumped NMR (OPNMR) phenomenon in GaAs is a striking example of a macroscopic observation in need of explanation. A recent finding¹³ showed that the photoconductance and the OPNMR signal followed a similar spectral dependence. Figure 1 compares these NMR data, the average of signals for left and right photon helicities from Ref. 4, with our photoconductance data taken with linear polarized light, both at 9.4 T and ~ 10 K. A salient feature is that both phenomena exhibit a peak near 1.5 eV. Previously, several explanations for the peak in the OPNMR intensity were suggested, for example, that 1.5 eV light is resonant with exciton or shallow-donor transitions (which have been proposed as electronic species that polarize nuclei), or that 1.5 eV light is somehow better at populating these electronic states than other photon energies because of relaxation issues. Rather, the correlation shown in Fig. 1 encouraged us to seek a simple, quantitative model for OPNMR that was based on understanding the photoconductance.

II. EXPERIMENT

OPNMR and photoconductance experiments were performed at 9.4 T magnetic field on samples that were 350 μm thick, with surface orientation of [100], with resistivity greater than $10^7 \Omega \text{ cm}$, and with mobility greater than $6000 \text{ cm}^2/\text{V s}$, from AXT, Inc. OPNMR data were collected using the saturation-recovery experimental protocol described previously.⁴ For photoconductance measurements,¹³ 1 V dc was applied across copper clamps that contacted annealed indium layers, which had been deposited on the GaAs as 0.5 μm thick films. This established an electric field inside the GaAs perpendicular to both the magnetic field and the laser propagation direction. The contacts were 5 mm apart, and the laser illuminated a region 3 mm in diameter between the contacts. In the dimension perpendicular to both the electric and magnetic fields, the GaAs sample was cut so that it was no wider than the laser spot. The light transmis-

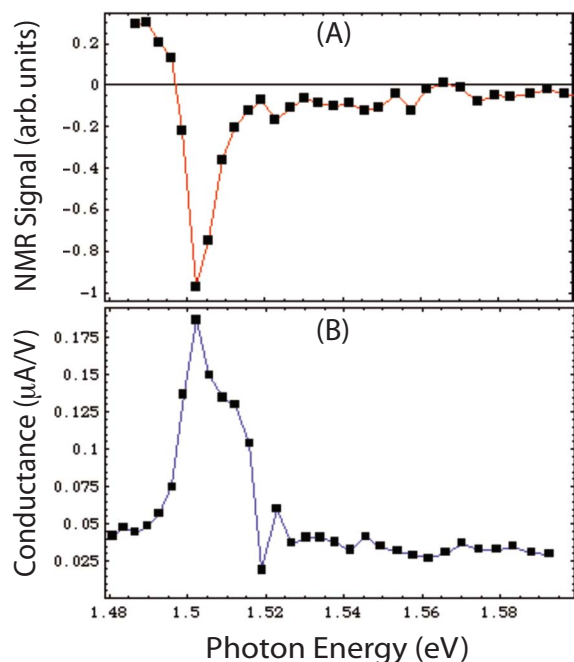


FIG. 1. (Color online) Comparison of two optical phenomena near the band gap of GaAs, (A) ^{69}Ga NMR enhancement (Ref. 4) and (B) photoconductance, both with linear polarized light, 9.4 T, and ~ 10 K.

sion fraction through our cryostat windows was measured to be ~ 0.7 , independent of the laser power, and it was estimated from the GaAs refractive index that 0.68 of this light penetrated into the GaAs. This gave an overall transmission fraction of ~ 0.5 , which was used for quantitative modeling of the data.

III. EXCITATION AND RECOMBINATION MODEL

For the modeling, our approach was to combine literature absorption data with simple rate expressions for charge-carrier recombination, as was done recently for NMR enhancements in crystalline silicon.⁹ Literature absorption data, taken at low temperature, exist for semi-insulating GaAs at low magnetic field¹⁴ and for molecular beam epitaxy (MBE) grown GaAs at high magnetic field.¹⁵ We have concatenated the two data sets such that the semi-insulating data were used below the band gap, where absorption from defects dominates, and the MBE data were used above the gap, where presumably band-to-band transitions dominate. The two sets were joined at the exciton peak, requiring the semi-insulating data to be shifted slightly to higher energies with higher magnetic field. The fact that absorption from impurities into the band should increase slightly in energy with increasing magnetic field provides motivation for applying this shift. Figure 2 shows the absorption coefficients at low field, 4, and 10 T, that were used as an input to the model.

The optical excitation process was modeled by allowing for two pathways of charge-carrier recombination: one at crystalline defects, whose rate is first order in the carrier concentration, and the other with another free carrier, whose

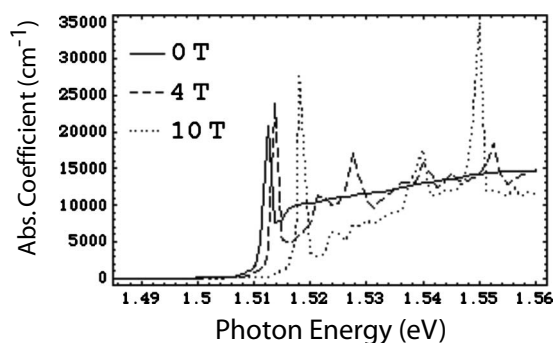


FIG. 2. Absorption coefficients for GaAs at low temperature for three different magnetic fields used as an input to our model.

rate is second order in the carrier concentration. Both processes are likely important for near-band-gap laser irradiation. Photobleaching and charge-carrier diffusion were ignored. Thus, in this model, a volume element reaches a steady condition when its rate of carrier trapping has matched the rate of carrier generation inside it:

$$k_1 N n + k_2 n^2 = G(z). \quad (1)$$

Here, N and n are the concentrations of defect traps (assumed constant) and free electrons, respectively. For a photon flux decaying exponentially with the depth z into the wafer, $\phi = \phi_0 e^{-z/\lambda}$, the generation rate of free electrons in the volume element is

$$G(z) = -\frac{\gamma d\phi}{2 dz} = \frac{\gamma \phi_0}{2\lambda} e^{-z/\lambda}, \quad (2)$$

where λ is the depth at which the photon number is reduced by $1/e$, or roughly speaking, the light penetration depth, and $\gamma \approx 2$ is the average number of charge carriers released per absorption event.²⁶ Implicit in this model is the approximation that the concentrations of free electrons and free holes are equal at every point (equivalent to assuming particle-antiparticle symmetry for both generation and trapping). Solving for the concentration of free electrons:

$$n(z) = \frac{k_1 N}{2k_2} [\sqrt{1 + C_1 G(z)} - 1], \quad (3)$$

where $C_1 = 4k_2 / (k_1 N)^2$ is a measure of second-order recombination relative to first order. To predict the electrical conductance under the experimental conditions of Fig. 1, we assume that the applied electric field is uniform over the irradiated volume (valid because the contact separation is much bigger than the wafer thickness), and that the light gets only one pass through the wafer. The conductance is then given by

$$\text{Conductance} = (\mu_e + \mu_h)eA/L^2 \int_0^T n(z)dz \quad (4a)$$

$$= \frac{C_2}{2} \int_0^T [\sqrt{1 + C_1 G(z)} - 1] dz \quad (4b)$$

$$= C_2 \lambda \left\{ \ln \frac{1 + \sqrt{1 + C_1 G_o e^{-T/\lambda}}}{1 + \sqrt{1 + C_1 G_o}} + \sqrt{1 + C_1 G_o} - \sqrt{1 + C_1 G_o e^{-T/\lambda}} \right\}, \quad (4c)$$

where T is the wafer thickness, L is the contact separation, A is the laser spot area, $G_o = \gamma\phi_o/2\lambda$, $C_2 = (\mu_e + \mu_h)eAk_1N/k_2L^2$, μ_e and μ_h are the electron and hole mobilities (assumed independent of λ), and e is their charge magnitude in Eq. (4a). The integral solution is shown to demonstrate that in this model, the dependence of the conductance on ϕ_o and λ can be written explicitly.

Plots of the conductance versus penetration depth are shown in Fig. 3, for various laser intensities [Fig. 3(A)] and wafer thicknesses [Fig. 3(B)], taking $C_1 = 2 \times 10^{-17} \text{ s cm}^3$. There exists an optimal penetration depth because of a battle between losing photons out through the back of the wafer, and confining the electron-hole gas to smaller volumes, thus increasing the second-order recombination rate. (A model without second-order recombination does not predict an optimum.) Optimal penetration depths, λ_{opt} , for various intensities and wafer thicknesses are plotted in Fig. 3(C). The largest conductivities are predicted when the wafer thickness is about three times the penetration depth, although it depends slightly on the intensity. The optimal penetration depth shifts to longer values for higher intensities, since alleviating the second-order recombination becomes more important than losing photons.

Since the absorption data map each photon energy onto a penetration depth, it is a simple matter to predict the photon-energy dependence of the conductance. Figure 4 shows a comparison between theory and experiment. We get good agreement with only one adjustable parameter, C_1 , determining the shape of the theoretical curve (C_2 is just a multiplicative factor). The value obtained from data fitting for $C_1 = 2 \times 10^{-17} \text{ s cm}^3$ is within an order of magnitude of the value computed from the literature,¹⁶ $3 \times 10^{-18} \text{ s cm}^3$. The present model predicts the peak just below the band gap as well as the dip at $\sim 1.52 \text{ eV}$ due to strong exciton absorption. To reiterate in terms of photon energy, at low energies photons are being lost, at high energies the excited carriers recombine faster, and the balance gives rise to a peak in the conductance near 1.5 eV.

IV. NUCLEAR POLARIZATION MODEL

A. Free electron model

The most elementary model for the OPNMR signal intensity would suggest that the nuclear polarization rate follows the number of free electrons precisely. The recombination

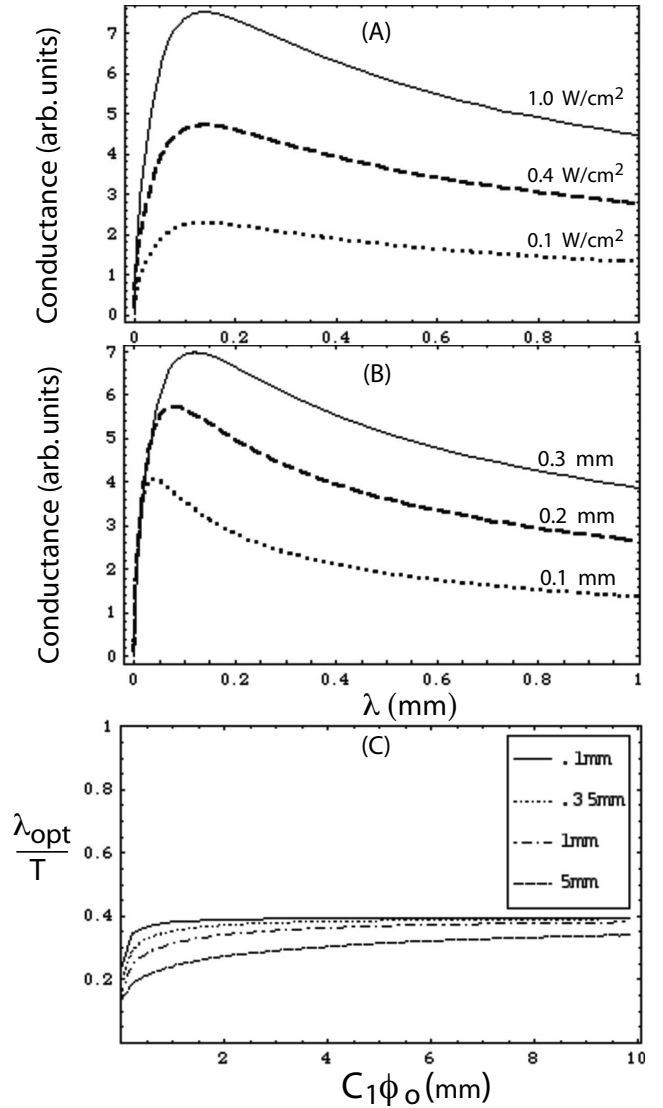


FIG. 3. (A) Conductance versus penetration depth for several laser intensities (in W/cm²) with the thickness fixed at 0.35 mm, and (B) for several thicknesses with the laser intensity fixed at 1 W/cm². (C) Optimal penetration depth versus laser intensity (more precisely $C_1\phi_o$) for various thicknesses.

model above yields the spectral dependence of the number of free electrons, thus affording a prediction for the spectral dependence of OPNMR. Indeed, a reasonable fit of the NMR data is obtained under this assumption of spatially uniform nuclear polarization, as shown in Fig. 5 (“Theory 1”). However, there is experimental evidence for nonuniform nuclear polarization,¹⁰ and there is reason to believe that the steady-state electron-spin polarization could be different at different photon energies. We incorporate the latter effect now.

If it can be assumed that spin exchange rapidly equilibrates the localized and delocalized excited electrons,¹⁷ then all excited electrons can be thought of as one reservoir with a single spin-lattice relaxation time T_{1e} and a single recombination time τ . Since the nuclear polarization rate scales with the departure of the electron-spin polarization from equilibrium, $\Delta S = \langle S_z \rangle - S_{eq}$, one can write the following proportionality for the case of rapid spin exchange:

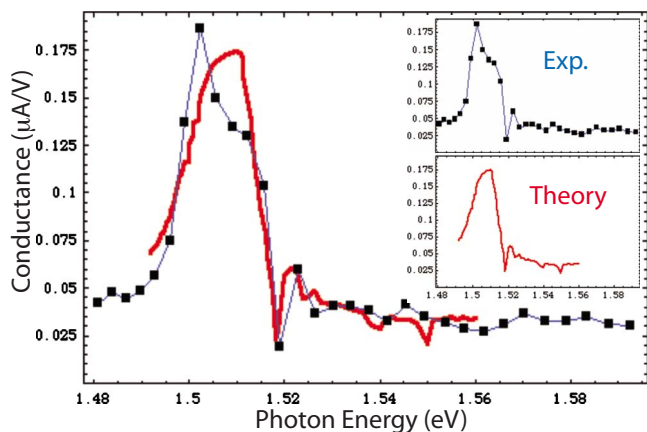


FIG. 4. (Color online) Experimental and theoretical photoconductances overlaid, separate in inset, for 350 μm thick GaAs at 10 T field, 10 K, and 70 mW laser power.

$$\text{nuclear polarization} \propto \Delta S = \frac{S_o - S_{eq}}{1 + \tau/T_{1e}}$$

regardless of which electronic reservoir is doing the polarization. The right-hand side can be derived from a simple rate analysis. For linearly polarized light, the initially excited polarization is $S_o=0$, so optical nuclear polarization is opposite in direction to thermal nuclear polarization. (That is what is meant by negative NMR signal.) The overall recombination rate can be found from Eq. (3) by taking $G(z)/n(z)$:

$$\frac{1}{\tau} = \frac{k_1 N}{2} [1 + \sqrt{1 + C_1 G(z)}],$$

and it depends on the penetration depth through $G(z)$. Over the relevant photon-energy range, τ changes by about 1 order of magnitude; thus, we would also expect the electron-spin departure to change. Figure 6 plots the relative electron-spin departure versus photon energy, for a value of $C_3=k_1NT_{1e}=0.5$, which is the value determined from our hyperfine shift data (see below). Including this effect into the free electron

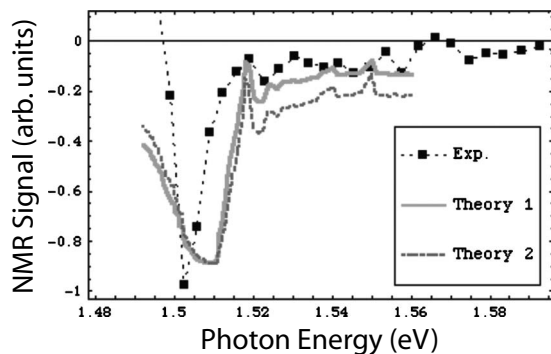


FIG. 5. ^{69}Ga OPNMR signal for 350 μm thick GaAs at 10 T field, 10 K, and 320 mW laser power. Experimental points are squares. Overlaid are predictions from an oversimplified free electron model (Theory 1) and a free electron model accounting for the energy-dependent electron-spin polarization (Theory 2).

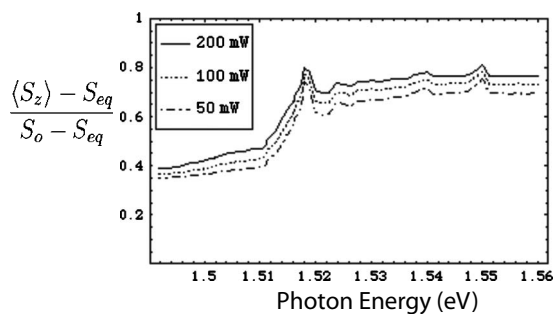


FIG. 6. Theoretical steady-state departure of the electron-spin polarization from equilibrium (relative to the initially excited departure) versus photon energy, for various laser powers.

model for nuclear polarization makes the fit *worse*, as can be seen in Fig. 5 (“Theory 2”). Already, with the simple free electron model (“Theory 1” in Fig. 5), we were overestimating supergap signals relative to the subgap ones. Since electrons recombine faster with supergap irradiation, their steady-state spin departure is higher, and thus, inclusion of this effect causes the theory to weight supergap enhancements to an even greater degree. For this, and other reasons, we consider a nuclear polarization mechanism based on localized electrons.

B. Shallow-donor model

It was suggested many years ago that optical alignment of bulk nuclear spins in GaAs occurs because of fast cross-relaxation of nuclei with electron spins at localized centers and subsequent magnetization transport by nuclear-spin diffusion.^{19,20} The localized centers were presumed to be donors because the hole wave function at the top of the valence band has a node at the nucleus and, thus, interacts weakly, and furthermore, because hole spins relax quickly with the lattice. The relevant donors were proposed to be shallow in energy below the conduction band because the sign of their g factor is consistent with the sign of the NMR enhancement, their weak binding energy allows the electron to hyperfine-contact thousands of nuclei simultaneously, and direct evidence of optical nuclear polarization in the vicinity of these donors has been obtained.¹⁹ The possibility that deep donors also participate in the spin dynamics has not been ruled out. This shallow-donor model has been used to fit the magnetic-field dependence of the optical Overhauser effect⁵ by noting that the cross-relaxation rate picks off the spectral density, approximately at the electron’s Larmor frequency, ω_e :

$$\frac{1}{T_1} = e^{-4r/a_0} \frac{F a_n^2 \gamma_c}{1 + \omega_e^2 / \gamma_c^2} = \frac{e^{-4r/a_0}}{T_{1,0}}. \quad (5)$$

Here, a_0 is the decay length of the donor wave function (which shrinks nonspherically with magnetic field, although it is approximated as constant here), F is the time-averaged donor occupation fraction, a_n is the strength of the hyperfine Hamiltonian at the donor center, γ_c is the decay rate for the correlation of the hyperfine Hamiltonian, and $T_{1,0}$ is the characteristic cross-relaxation time at the donor center.

In light of several apparent inconsistencies with the shallow-donor model, recent OPNMR data were interpreted in the context of delocalized electrons.^{4,10} The major argument was that two short-irradiation-time predictions of the shallow-donor model were not observed experimentally: nonlinear NMR signal-growth kinetics, and hyperfine shift and broadening of the NMR line. The latter was recently discovered at 4.7 T,¹⁸ although no evidence of this was seen at 9.4 T.⁴ We discuss shifts later in the paper and consider first the issue of signal-growth kinetics.

In the shallow-donor model, nuclear polarization, $\langle I_z \rangle$, evolves in space-time according to a generation-diffusion equation¹⁹ (ignoring nuclear spin-lattice relaxation):

$$\frac{\partial C}{\partial t} = \frac{e^{-4r/a_0}}{T_{1,0}}(1 - C) + \frac{D}{r^2} \frac{\partial}{\partial r} r^2 \frac{\partial C}{\partial r}, \quad (6)$$

where $C = \langle I_z \rangle / I_s$, I_s is the polarization that the nuclei would relax to if there was no spin diffusion or spin-lattice relaxation, and D is the spin diffusion coefficient. $T_{1,0}$ is given by Eq. (5), where, in our model, we take F to increase with the concentration of free electrons according to a saturation curve:

$$F = \frac{n}{n + n_s}, \quad (7)$$

where n_s is the concentration corresponding to $F = 1/2$. This equation can be derived under assumptions similar to what Langmuir made for the adsorption of a classical gas onto a fixed number of sites.²¹ Explicitly, one sets the rate of binding equal to the rate of ionization and solves for F .

Our theoretical curves were generated by solving Eq. (6) in radial coordinates, with the nuclear polarization fixed to be zero at some very large radius. This isolated-impurity approach should be valid for irradiation times less than the time scale for nuclear spin to diffuse between shallow donors, which for ⁷¹Ga is $\sim d^2/D \sim 100$ s, where d is half the impurity separation for samples with a shallow-donor concentration of 10^{15} cm^{-3} .²² For comparison, we also solved Eq. (6) in rectangular coordinates with zero-flux boundary conditions at the walls of a rectangular box enclosing the impurity. This allowed us to simulate the presence of neighboring impurities. Varying the three dimensions of the box and the three coordinates of the impurity within the box, each independently, also allowed us to simulate disorder in the impurity spacing. The effect of neighboring impurities on the kinetics of NMR signal growth was very small for at least 2 min of irradiation, the growth remaining highly linear even when appreciable nuclear polarization built up at the impurity-impurity boundary. Hence, the isolated-impurity solution provided a good approximation for simulating NMR signal growth over the time scale of several minutes.

When solving Eq. (6), it is crucial to adjust Paget's value¹⁹ of $T_{1,0}$ to the relevant conditions of one's experiment. Paget measured NMR optically by detecting a drop in the luminescence polarization through the nuclear Hanle effect. In his photoluminescence experiment, he focused the incident light down to a small spot of very high intensity, with photons whose energy was far above the band gap, where the

penetration depth is extremely thin. Within such a small irradiation volume, the shallow donors were completely filled. Such is not the case for many of the bulk OPNMR experiments that have been carried out in the past two decades. Furthermore, the high magnetic field necessary for induction-coil NMR has the effect of reducing the spectral density at the electron's Larmor frequency by 1 or 2 orders of magnitude, as compared to Paget's experiment. For both of these reasons, Paget's value of 80 ms significantly underestimates $T_{1,0}$ in typical bulk OPNMR. It turns out, as we show below, that the mystery associated with nonlinear kinetics is rooted in this discrepancy. Our model predicts linear kinetics for high field, low intensity, and sub-band-gap irradiation, the conditions under which the experiment is typically performed.

Equation (6) has two limiting cases: the diffusion-limited regime and the cross-relaxation-limited regime. These regimes have been investigated for paramagnetic defects dipole coupled to nuclei,²³ and the same principles apply here. In the diffusion-limited regime, one expects nonlinear kinetics because the rate of signal growth is proportional to the diffusional driving force at the interface between the donor and the bulk. Initially, nuclear polarization builds up rapidly within the donor, and there is a large gradient in polarization at the donor-bulk interface. As the bulk nuclei get polarized (by diffusion), the driving force for polarization injection goes down. Hence, the signal grows with a concave down time dependence in this diffusion-limited regime.

The dimensionless parameter $\zeta = 16DT_{1,0}/a_0^2$ can be compared to unity to determine the system's regime.¹⁰ For OPNMR at 9.4 T and 30 mW/mm^2 of laser intensity, we find $\zeta \sim 20$, indicating cross-relaxation limitation. In this case, where diffusion is fast, C stays small for all radii, particularly for short times. Under these conditions, Eq. (6) becomes

$$\frac{\partial C}{\partial t} = \frac{e^{-4r/a_0}}{T_{1,0}} + \frac{D}{r^2} \frac{\partial}{\partial r} r^2 \frac{\partial C}{\partial r}. \quad (8)$$

The dimensionless signal, S (total nuclear angular momentum), is found by integrating C over the volume near the donor, then summing over all donors

$$\frac{dS}{dt} = \int_0^T dz (N_d A \Delta S) \int_0^\infty dr (4\pi r^2) \frac{e^{-4r/a_0}}{T_{1,0}}, \quad (9)$$

where N_d is the shallow-donor concentration. The right-hand side is independent of time. Thus, in the cross-relaxation-limited regime, one expects linear kinetics at short times. An interesting aside is that the growth rate is independent of the nuclear-spin diffusion coefficient.

Consistent with the analytical result of Eq. (9), Fig. 7(A) shows a plot of the predicted time dependence from our model, which numerically solves Eq. (6) and accounts for the spatial dependence of photon flux, overlaid onto data from Ref. 4, both at 1.503 eV, 320 mW, and 9.4 T. Figure 7(B) shows the theoretical curve at the same magnetic field but at 1.55 eV, the photon energy corresponding to the thinnest penetration depth ($< 1 \mu\text{m}$), where the nonlinearity is expected to be greatest. That is linear as well.

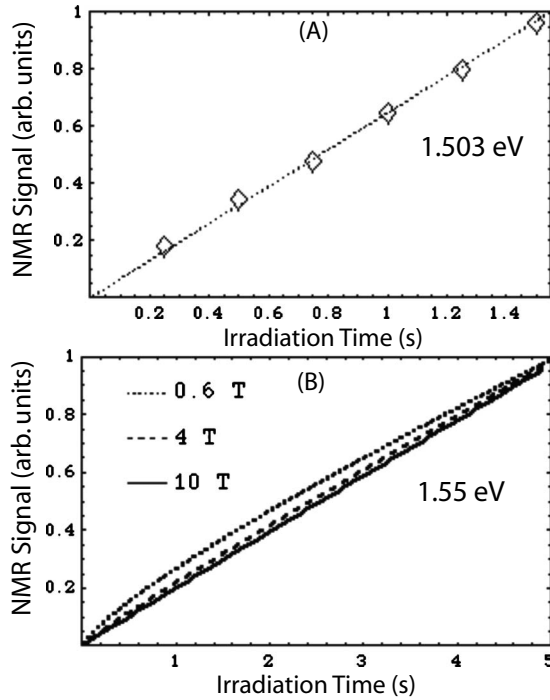


FIG. 7. (A) Comparison of the theoretical and experimental ^{71}Ga OPNMR signal growth for short irradiation times at 1.503 eV, 320 mW, and 9.4 T. (B) Theoretical ^{71}Ga signal growth at 1.55 eV, 320 mW, and several different magnetic fields. Curves corresponding to 4 and 10 T are multiplied by factors of 2.8 and 12.2, respectively, to easily see the difference in curvatures at different magnetic fields.

On the other hand, our calculations suggest that it could be possible to push the system into the diffusion-limited regime, and observe nonlinear kinetics. One's best chances would be at low magnetic field, as can be seen from Fig. 7(B) or Eq. (5), as well as at high photon energy and flux. This would be an important test of the shallow-donor mechanism.

In the context of the shallow-donor model, we return to the photon-energy dependence of OPNMR. In addition to the recombination parameters that were fixed by the photoconductance fit, there are two new fitting parameters: one determining the electron-spin polarization (C_3) and the other determining the donor occupation fraction (n_s). These parameters were determined iteratively, like how one tightens a car tire's bolts, by gradually improving the fit of three data sets: OPNMR versus photon energy, OPNMR versus laser power (shown in the next section), and hyperfine shift versus irradiation time (shown in Sec. V C). With $C_3=0.5$ and the donor occupation fractions shown in Fig. 8(B), one can see a better fit of the photon-energy dependence in Fig. 9 as compared to the free electron model. The better fit arises from saturation of donor occupation, which decreases supergap enhancements relative to subgap ones. The disagreement for photon energies below 1.5 eV is due to the onset of an opposing polarization mechanism, perhaps related to deep defects,⁴ which this model does not attempt to account for.

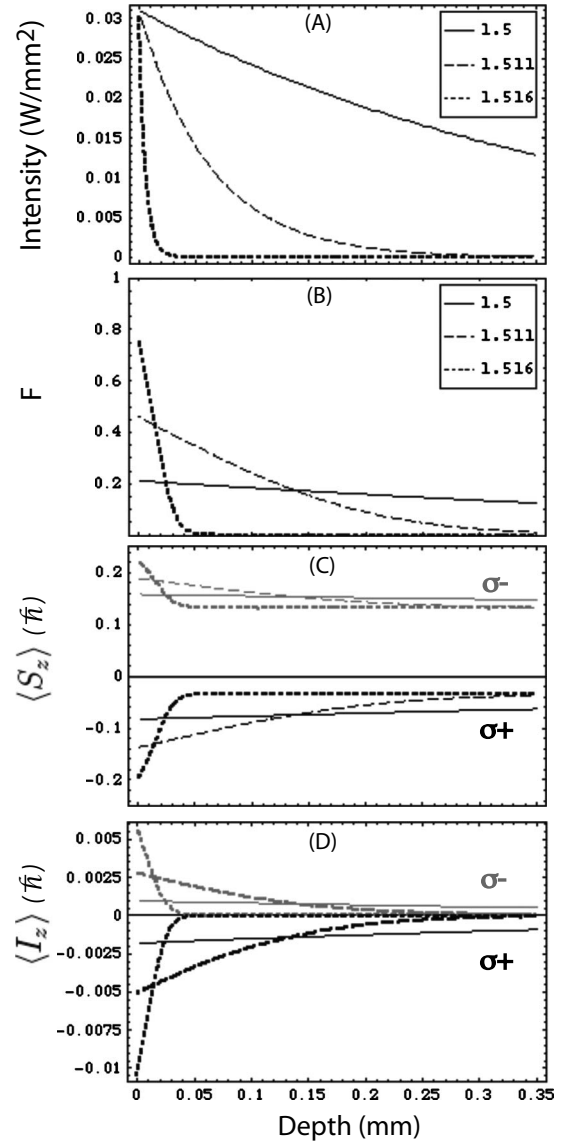


FIG. 8. Predicted decay of (A) laser intensity, (B) donor occupation fraction, (C) electron-spin polarization, and (D) ^{71}Ga nuclear-spin polarization with depth into the crystal. Curves are shown for three photon energies (in eV, same for all four plots), for 320 mW of laser power, and for 20 s of irradiation, at 10 T field and 10 K.

V. PREDICTIONS

A. Laser intensity dependence

In addition to the dependence of OPNMR on photon energy, irradiation time, and magnetic field, the present model makes predictions for the dependence on laser intensity. Researchers have modeled the intensity dependence of OPNMR previously in InP (Ref. 24) and CdTe (Ref. 8) with an empirical formula. It was hypothesized²⁴ that the nuclear-spin polarization inside some volume scales with $1 - \exp(-I/I_s)$, where I is the impinging intensity on that volume and I_s is some saturation intensity. By physical reasoning, since the nuclear spins do not interact directly with near-band-gap photons, the nuclear polarization should actually depend on

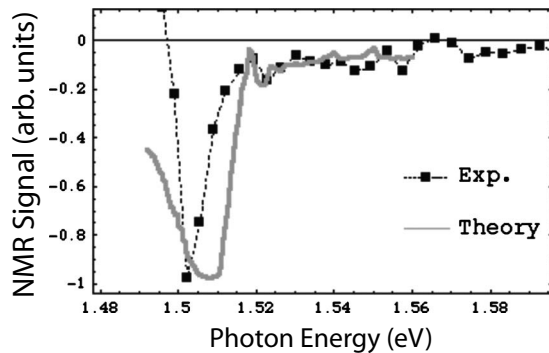


FIG. 9. Theoretical ^{69}Ga OPNMR signal versus photon energy, assuming the shallow-donor polarization mechanism, overlaid onto experimental data from Ref. 4.

G/G_s , which is the generation rate of free electrons relative to its saturation value. Replacing I/I_s with G/G_s in the above empirical formula and using Eq. (2), one finds that I_s should scale with λ . Thus, while previous bulk OPNMR studies have quoted a saturation intensity for the semiconductor, in actuality, this saturation intensity is not unique, and depends on the penetration depth of the light.

Equation (4c) shows the variation of the photoconductance with photon flux (or laser intensity); it seems reasonable to consider the photoconductance as a first-order model for the OPNMR signal. Taking Eq. (4c) as a first-order model (up to a constant) for the OPNMR signal, we expand this equation in a power series of the laser intensity:

$$\begin{aligned} \text{OPNMR signal} \\ = \frac{C_1}{4}(1 - e^{-T/\lambda})I_o - \frac{C_1^2}{32\lambda}(1 - e^{-2T/\lambda})I_o^2 + O(I_o^3). \end{aligned} \quad (10)$$

Two noteworthy features of this model are as follows:

(1) The NMR signal is predicted to grow linearly with intensity for low intensity, the slope being independent of penetration depth for a thick wafer.

(2) The onset of nonlinear growth is suppressed for longer penetration depths.

Both of these features are evident in the experimental data. In Fig. 10, we show the laser-power dependence of the ^{71}Ga NMR signal, built up for 2 min of optical irradiation, for two subgap photon energies. Negative NMR signal implies that the nuclear polarization is inverted relative to the thermal-equilibrium polarization. One can see initial linear growth with the same slope for the two different energies (penetration depths), and deviation from linearity occurring first for the shorter penetration depth.

Our theoretical curves, generated by considering all effects discussed thus far (recombination kinetics, electron-spin polarization, and donor filling), are also shown in Fig. 10. The data are fitted well provided that the theory is shifted in energy by ~ 6 meV. The same shift is seen in the subgap photon-energy dependence in Fig. 9, the experimental and predicted peaks occurring at 1.502 and 1.508 eV, respectively. This discrepancy is likely rooted in incorrect values of the absorption coefficient for our sample. In fact, we applied a 6 meV shift to the subgap absorption data to account for

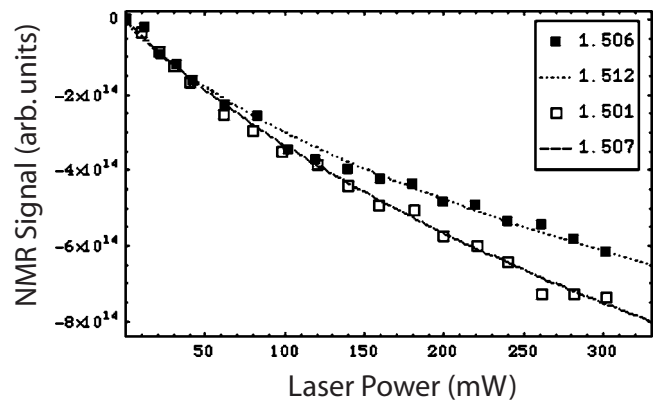


FIG. 10. Experimental dependence of ^{71}Ga NMR signal on laser power for 1.501 eV (open squares) and 1.506 eV (filled squares) photon energies. Theoretical curves, shifted in energy by 6 meV, are overlaid.

the magnetic field, so this, precisely, may be the problem. (It is not obvious how to adjust subgap absorption data since both the band gap and defect binding energies change with magnetic field.)

At this point, our model is complicated enough such that it is difficult to tell what exactly is responsible for the deviation from nonlinear growth with intensity. While we have discussed second-order recombination of charge carriers, one would expect a similar deviation from linearity due to filling of shallow-donor sites. In fact, we found that we could fit the CdTe and InP data using a simple shallow-donor filling formula, $(G/G_s)/(1+G/G_s)$, just as well as the empirical formula. (They have very similar Taylor expansions.) On the other hand, we could also fit these data considering only the recombination model in Eq. (10), although not quite as perfect. Therefore, it is unclear from the literature data on bulk OPNMR in CdTe and InP whether the nonlinearity is from second-order recombination or from filling of shallow donors. It is also unclear from the GaAs data in Fig. 10. These data are in the intensity regime where the first two terms of the Taylor expansion are the largest contributors, and in that case, the two theories can be made to fit the same data.

The data in Fig. 11 resolve this issue for GaAs. Here, we show the NMR enhancement *leveling off* in the high intensity regime. (These data are over a similar laser-power range as Fig. 10, but the beam is narrower, thus, higher in intensity.) Any reasonably simple model in which the nuclei are polarized by delocalized electronic species cannot account for this saturation effect. In the context of the present model, the leveling off corresponds to complete filling of the shallow-donor sites within the irradiation volume.

Local heating is a concern. We have calibrated that the sample temperature is raised by ~ 8 K for 100 mW of incident laser power. It is possible that each increase in irradiation power provides a detrimental thermal effect that exactly cancels the expected increase in nuclear polarization rate, leading to a flat line. Such a scenario seems extremely unlikely considering the saturation effect was observed at five different photon energies. Furthermore, calibration suggests that, for the data in Fig. 11, the sample temperature stayed

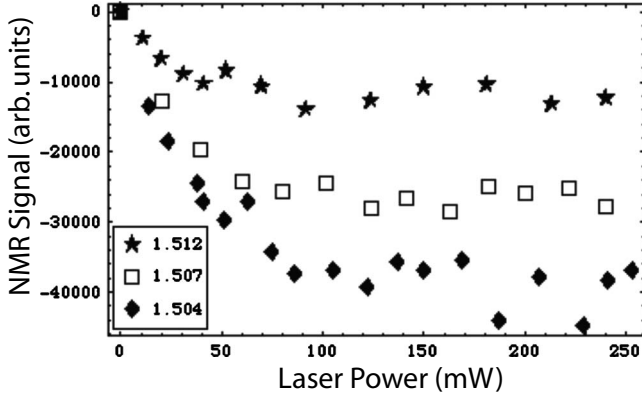


FIG. 11. Reproduction of the data in Fig. 10, but at higher laser intensities (narrower beam). ^{71}Ga NMR data are shown for photon energies of 1.504, 1.507, and 1.512 eV. Similar-looking saturation curves were also observed at 1.509 and 1.511 eV.

approximately constant for laser powers ranging from 80 to 240 mW.

The data in Fig. 10 allow us to distinguish between two alternative formulas^{5,19} for the dependence of $T_{1,0}$ on F [Eq. (5)]. For irradiation at 1.5 eV at high field, we are in the cross-relaxation-limited regime, where the nuclear polarization rate scales with the cross-relaxation rate. For the proposal¹⁹ that this rate grows in proportion to F , one would expect the NMR signal to grow linearly with power for low powers. For the proposal⁵ that the rate grows with F^2 , one would expect the NMR signal to grow quadratically with (low) power. In Fig. 10, it appears there is no evidence of initial quadratic growth; thus, the data are consistent with the relaxation rate scaling with F .

B. Nuclear-spin temperature

The present model makes predictions for other bulk NMR quantities, such as the spin temperature (or spin polarization) of nuclei contributing to the NMR signal. The signal-weighted nuclear polarization is given by²⁵

$$\overline{\langle I_z \rangle}(t) = \frac{I(I+1)}{S(S+1)} \frac{\int dz \Delta S(z)^2 \int dr r^2 C(z,r,t)^2}{\int dz \Delta S(z) \int dr r^2 C(z,r,t)},$$

where $I=3/2$ for all nuclei in GaAs and $S=1/2$. In the cross-relaxation-limited case, this expression simplifies to the following for short times Δt :

$$\overline{\langle I_z \rangle}(\Delta t) \propto \Delta t \frac{\int dz F(z)^2 \Delta S(z)^2}{\int dz F(z) \Delta S(z)}.$$

One can use this proportionality to understand the photon energy and flux dependence of $\overline{\langle I_z \rangle}$ at short times. Figure 12(A) shows the predicted photon-energy dependence of $\overline{\langle I_z \rangle}$ for 2 s of irradiation with two different laser powers and

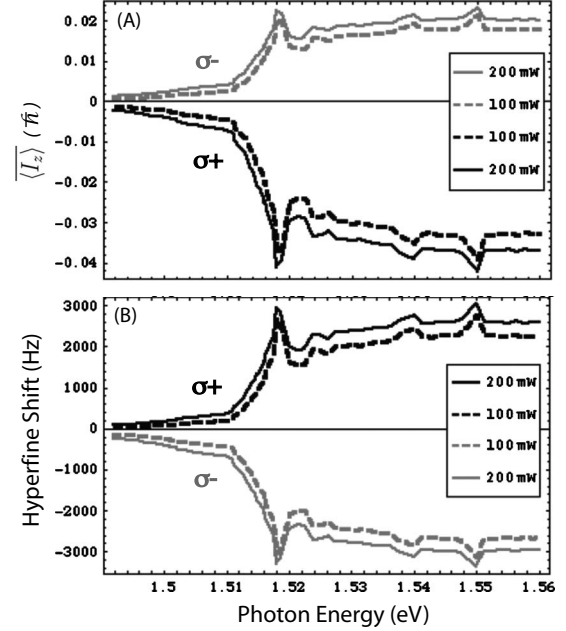


FIG. 12. (A) Average z component of ^{71}Ga nuclear angular momentum, in units of \hbar , for nuclei contributing to the NMR signal. (B) Light-induced hyperfine shift of the ^{71}Ga NMR line. Predictions are shown as a function of photon energy, after 2 s of irradiation, for two different laser powers, and for both circularly polarized helicities, at 10 T and 10 K.

helicities. In our model, this quantity is greater for supergap irradiation because both the donor occupation fraction and the electron-spin departure are greater [see Figs. 8(B)–8(D)]. Experimental verification of this prediction would confirm the physical picture presented here. At low energies, there are many polarization centers in the irradiation volume, but individually, they are weakly polarized. At high energies, the opposite is true. So there is a battle between quantity and quality, or between the number of nuclei and the degree to which they are polarized. This prediction has yet to be verified for GaAs, but is consistent with InP experiments.⁶

Figure 13(A) shows the predicted laser-power dependence. At the highest laser powers and the highest photon energies, the power dependence of the average nuclear-spin polarization is predicted to level off. This corresponds to filling up all of the donor sites within the irradiation volume.

C. Hyperfine shift

As mentioned earlier, a predicted yet elusive OPNMR quantity, the NMR frequency shift due to the hyperfine field from spin-polarized electrons, was finally observed, in a 4.7 T magnet.¹⁸ The discoverers modeled the time dependence of this shift, and their theoretical curves qualitatively matched their data. Our laboratory searched for and recently found this shift at 9.4 T; the data are shown in Fig. 14. Each data point represents the central frequency of a Gaussian fit to the NMR line, with the laser left on the sample during NMR acquisition. Overlaid onto the data are the predicted curves from our model, calculated using the following for-

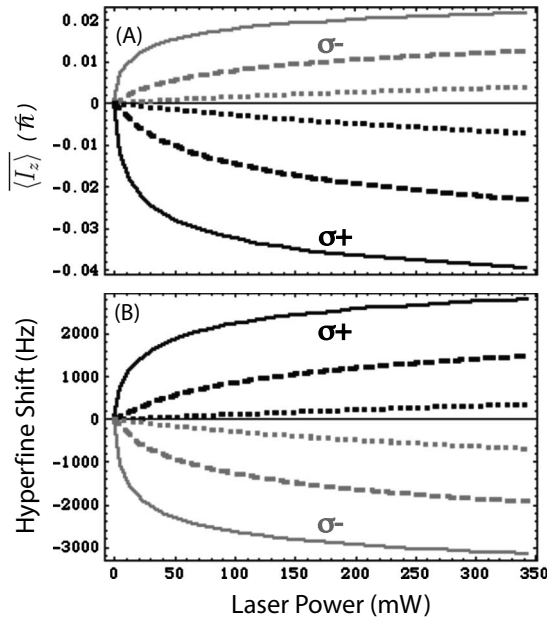


FIG. 13. (A) Average z component of ^{71}Ga nuclear angular momentum, in units of \hbar , for nuclei contributing to the NMR signal. (B) Light-induced hyperfine shift of the ^{71}Ga NMR line. Predictions are shown as a function of laser power, after 2 s of irradiation, for three different photon energies: 1.502 eV (short dashes), 1.515 eV (long dashes), and 1.558 eV (solid line), and for both circularly polarized helicities, at 10 T and 10 K.

mula for the average hyperfine shift of the ^{71}Ga NMR frequency:

$$\overline{\Delta\nu} = (-169 \text{ kHz}) \frac{\int dz F \langle S_z \rangle \Delta S \int e^{-2r/a_0} C(z, r, t) r^2 dr}{\int dz \Delta S \int C(z, r, t) r^2 dr}.$$

An asymmetry in the shift with respect to the light helicity, due to partial relaxation of the electron spins toward a Boltzmann population of the Zeeman levels, can be seen in both the data and the predictions. Also, one can see that the experimental helicity-dependent shifts do not fully decay to zero at long times, which is true when the laser is both unblocked and blocked during NMR acquisition. This slight memory of the light helicity in the dark is likely due to the nuclear-nuclear dipole field, although further experiments are needed to confirm this.

The data in Fig. 14 allowed the value of the fitting parameter $C_3 = k_1 N T_{1e}$ to be uniquely determined: 0.5 ± 0.2 . The model presented here, which is constrained to fit the photon-energy dependence of both the photoconductance and the OPNMR signal, and the laser-power dependence of the OPNMR signal, agrees with the hyperfine shift data quantitatively. This agreement may be fortuitous, since the model does not account for the expected shrinkage of the shallow-donor wave function with magnetic field, which would decrease the time scale for the shift to decay off. It is interesting to note that this time scale is indeed shorter at 9.4 T

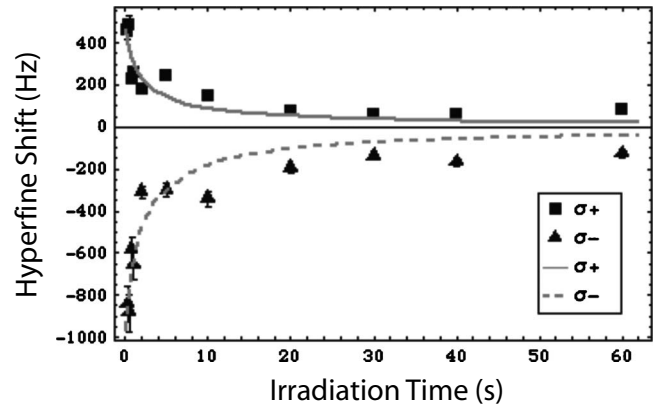


FIG. 14. Light-induced shift of the ^{71}Ga NMR frequency versus time of irradiation with 1.509 eV, 123 mW, and circularly polarized light. Theoretical curves are overlaid onto the data.

(~ 30 s) as compared to that at 4.7 T (~ 200 s).

In the present model, predictions for the dependence of this shift on photon energy and laser power are possible. Respectively, these dependences are shown in Figs. 12(B) and 13(B) for the two circularly polarized helicities. There are two effects which make the hyperfine shift (and thus hyperfine broadening, since it is a source of inhomogeneous broadening) significantly more noticeable for energies above the band gap:

(1) The higher donor occupation fraction leads to a greater time-averaged hyperfine field on the nucleus.

(2) The faster electron recombination does the same, but by preserving the initially excited electron-spin polarization.

For 1.505 eV and σ^+ light, the experimental conditions in Ref. 4, the hyperfine shift is predicted to be very small, which may explain its lack of observation in this reference. Like the OPNMR signal and the signal-weighted $\langle I_z \rangle$, the hyperfine shift is predicted to saturate at high laser powers, primarily because of donor filling.

VI. CONCLUSIONS

In summary, we set out to model the photon-energy dependence of GaAs OPNMR with simple recombination equations and literature absorption data, having been inspired by a correlation between the NMR and the photoconductance. We fit the major features of the photoconductance versus photon energy, noting that second-order recombination was necessary to explain the falloff at high energies. This fit allowed us to immediately predict the photon-energy dependence of OPNMR, assuming nuclear polarization by free electrons. The prediction qualitatively followed the data, but overestimated supergap enhancements relative to subgap ones, particularly when we accounted for electron-spin relaxation. Incorporating the fact that the relevant electronic reservoir could become filled, such as would be the case for shallow donors, allowed us to better fit the data.

Essentially, there are four numbers that parametrize the model presented above: two determining the recombination rate of optically excited electrons, one determining their par-

tioning onto shallow donors, and one determining their steady-state spin polarization. The first two were found from fitting the photoconductance data, and the latter two from fitting the NMR data. Thus, the model is fully constrained.

The penetration depth model presented here predicted that the NMR signal should deviate from linear growth with laser intensity, and that this deviation would onset sooner for shorter penetration depths. These facts were confirmed by the data, and theory and experiment agreed quantitatively, up to an energy shift that is likely due to incorrect absorption coefficients. Thus far, this is the most informative test of our model. (It was developed in order to explain the photon-energy dependence, but we did not have the intensity-dependence data at the time of its invention.)

There are two experiments, of particular importance, that one could perform to further test our penetration depth model. First, the average spin polarization of nuclei contributing to the NMR signal is predicted to be greater for photon energies above the band gap than below. Straining a GaAs wafer produces an electric field gradient at the nucleus and, thus, a quadrupolar splitting of the NMR line; the ratio of satellite-transition intensities provides a measure of the average nuclear-spin polarization,¹⁰ and thus, a means to test our prediction. Second, the hyperfine shift of the NMR line is likewise predicted to be significantly greater for photon energies above the band gap. Recently, it has come to our attention that Mui et al. performed these shift versus photon energy measurements, which agreed qualitatively with our predictions, and similarly agreed with their model's predictions.²⁷ This provides further justification for a penetration depth approach to understanding optical nuclear polarization.

Concerning the microscopics, we proved that the predicted signal-growth kinetics at high magnetic field is linear,

even for the shallow-donor mechanism, and thus, are not inconsistent with NMR data in the literature.^{5,4} Like the observations at 4.7 T,¹⁸ we observed a time-dependent shift of the optically pumped NMR frequency at 9.4 T. The decay of this shift was consistent with the shallow-donor nuclear polarization mechanism, and was quantitatively predicted by our model.

The model has also suggested additional experiments to test the nuclear polarization mechanism. While linear signal-growth kinetics is predicted at high field, it predicts that a slight buckling or curvature could be seen at low field if, in fact, bulk nuclei were polarized by spin diffusion out from impurities. Furthermore, for this mechanism, the model predicts that all experimental quantities related to OPNMR should saturate, i.e., cease growing with laser intensity at very high intensities. These include the NMR signal magnitude, the light-induced hyperfine shift, and the average nuclear-spin polarization. We have demonstrated, here, the NMR signal leveling off, for which the only explanation we can think of is the complete filling of the relevant electronic reservoir. This significantly increases our confidence that bulk nuclei are polarized by localized electrons. Experimental verification of the two other predictions, saturation of the hyperfine shift and the nuclear-spin polarization, would make our understanding of the optical nuclear polarization mechanism nearly complete.

ACKNOWLEDGMENTS

The authors acknowledge support from the National Science Foundation under project ECS-0608763. P.J.C. thanks Keshav Dani for offering experimental assistance, and acknowledges the NSF.

-
- ¹A. V. Overhauser, *Phys. Rev.* **92**, 411 (1953).
²T. R. Carver and C. P. Slichter, *Phys. Rev.* **102**, 975 (1956).
³G. Lampel, *Phys. Rev. Lett.* **20**, 491 (1968).
⁴A. K. Paravastu, S. E. Hayes, B. E. Schwickert, L. N. Dinh, M. Balooch, and J. A. Reimer, *Phys. Rev. B* **69**, 075203 (2004).
⁵P. L. Kuhns, A. Kleinhammes, T. Schmiedel, W. G. Moulton, P. Chabrier, S. Sloan, E. Hughes, and C. R. Bowers, *Phys. Rev. B* **55**, 7824 (1997).
⁶C. A. Michal and R. Tycko, *Phys. Rev. B* **60**, 8672 (1999).
⁷A. Goto, K. Hashi, T. Shimizu, S. Ohki, T. Iijima, and G. Kido, *Superlattices Microstruct.* **32**, 303 (2002).
⁸I. J. H. Leung and C. A. Michal, *Phys. Rev. B* **70**, 035213 (2004).
⁹A. S. Verhulst, I. G. Rau, Y. Yamamoto, and K. M. Itoh, *Phys. Rev. B* **71**, 235206 (2005).
¹⁰A. K. Paravastu and J. A. Reimer, *Phys. Rev. B* **71**, 045215 (2005).
¹¹M. N. Leuenberger, D. Loss, M. Poggio, and D. D. Awschalom, *Phys. Rev. Lett.* **89**, 207601 (2002).
¹²T. D. Ladd, J. R. Goldman, F. Yamaguchi, Y. Yamamoto, E. Abe, and K. M. Itoh, *Phys. Rev. Lett.* **89**, 017901 (2002).
¹³A. K. Paravastu, P. J. Coles, J. A. Reimer, T. D. Ladd, and R. S. Maxwell, *Appl. Phys. Lett.* **87**, 232109 (2005).
¹⁴M. D. Sturge, *Phys. Rev.* **127**, 768 (1962).
¹⁵P. Kner, S. Bar-Ad, M. V. Marquezini, D. S. Chemla, R. Lovenich, and W. Schafer, *Phys. Rev. B* **60**, 4731 (1999).
¹⁶Ren Guang-bao, Wang Zhan-guo, Xu Bo, and Zhou Bing, *Phys. Rev. B* **50**, 5189 (1994).
¹⁷D. Paget, *Phys. Rev. B* **24**, 3776 (1981).
¹⁸K. Ramaswamy, S. Mui, and S. E. Hayes, *Phys. Rev. B* **74**, 153201 (2006).
¹⁹D. Paget, *Phys. Rev. B* **25**, 4444 (1982).
²⁰C. R. Bowers, *Solid State Nucl. Magn. Reson.* **11**, 11 (1998).
²¹I. Langmuir, *J. Am. Chem. Soc.* **40**, 1361 (1918).
²²J. Lu, M. J. R. Hoch, P. L. Kuhns, W. G. Moulton, Z. Gan, and A. P. Reyes, *Phys. Rev. B* **74**, 125208 (2006).
²³W. E. Blumberg, *Phys. Rev.* **119**, 79 (1960).
²⁴R. Tycko, *Solid State Nucl. Magn. Reson.* **11**, 1 (1998).
²⁵A. K. Paravastu, Ph.D. thesis, University of California, Berkeley, 2004.
²⁶A more complicated model would consider the energy dependence of γ , being larger above gap than below gap by at most a factor of 2. The dynamic population of defects during illumination makes it difficult to obtain a functional form for this dependence. A simple approach would consider the dependence to

contain a single fitting parameter for the photoconductance, allowing one to weight the predicted above-gap conductance to a greater or lesser degree relative to the below-gap conductance. Already in our model, there exists such a parameter, C_1 , and a good fit is obtained by adjusting only its value to a final value which happens to be close to the literature value. This verifies our simple model, and the data would not even uniquely deter-

mine the energy dependence of γ in the more complicated model. Furthermore, the energy dependence of γ is a smaller effect than the energy dependence of the recombination rate, so it is neglected.

²⁷S. Mui, K. Ramaswamy, and S. E. Hayes *Phys. Rev. B* **75**, 195207 (2007).